JOURNAL OF SPACECRAFT AND ROCKETS
Vol. 33, No. 2, March–April 1996

In-Orbit Deployment Performance of Large Satellite Antennas

Akira Meguro*
Nippon Telegraph and Telephone Corporation, Kanagawa 238-03, Japan

Engineering Testing Satellite VI has been developed for advanced satellite communication experiments. It was launched from Tanegashima Space Center in August 1994. It failed to enter geostationary orbit because the apogee engine failed. However, the mission equipment remained fully functional, and the two large main reflectors and two small subreflectors were deployed successfully. The two main reflectors were 3.5 and 2.5 m in diameter. They were stowed against the tower structure during launch and deployed by spiral springs. Flight data from acceleration and temperature sensors were obtained. Of particular interest, the acceleration data agreed with the results of ground deployment and vibration testing. The deployment and vibration characteristics of the two large main reflectors are described and compared with the results of ground varification. In-orbit deployment and vibration characteristics are directly compared with the results of ground testing. Flight data obtained by in-orbit measurements show that ground validation methods are feasible and reliable.

Nomenclature

A	= amplitude of damping oscillation, m
c	= damping coefficient
f	= eigenfrequency of antenna structures during deployment, Hz
I	= moment of inertia, kgf m^2
k_θ	= spring constant equivalent to structural elasticity, N m/rad
L	= arm length between hinge point and an acceleration meter, m
ϕ, ψ, φ	= phase angles, rad
ω	= eigen-circular-frequency, rad/s

Introduction

BEGINNING with the Sakura series of communication satellites (CSs) in Japan, satellite communications complemented the terrestrial systems with functions such as the setting up of emergency circuits and communication with isolated islands. In recent years, the role of satellite communication has changed from being a supplementary system to being the main element of an advanced mobile communication system. For advanced satellite communication experiments, Engineering Satellite VI (ETS-VI) was launched by a Japanese H-2 rocket from Tanegashima Space Center on Aug. 28, 1994. ETS-VI was given the Japanese name Kiku-6 after rocket separation. Unfortunately, Kiku-6 was not put into geostationary orbit, because the satellite propellant system failed. However, primary events such as antenna deployment and solar-paddle deployment were successfully performed.

In-orbit deployments of satellite appendages are extremely critical events. Therefore, ground deployment tests and verification are indispensable for a successful mission. It took over 10 years to develop ETS-VI, and many test and/or verification procedures were performed. High mechanical and structural reliability was guaranteed, based on the results of ground deployment testing, vibration testing, acoustic testing, and so on. For the deployment characteristics in particular, the author suggested a new system identification method. It confirmed that deployment mechanisms maintained their as-designed performance through the assembling and testing processes.[1] The actual deployment characteristics must be measured in space and compared with the results of ground deployment tests.

There are some papers regarding the ground testing and the verification of satellite antennas.[2–4] However, the author could not find any paper describing the verification of ground deployment tests by in-orbit deployment characteristics. We can find valuable information only in failure reports such as that on the Galileo high-gain-antenna deployment anomaly.[5] Unfortunately, most anomaly reports are not published.

Any difference between the in-orbit deployment characteristics and the predicted deployment characteristics obtained by ground testing is significant in validating the ground verification methods. To measure the in-orbit deployment characteristics, one acceleration sensor was installed on the top of each main reflector. The sensors measure tangential acceleration instantaneously during deployment and after latchup. Deployment and vibration characteristics in the space environment can be obtained by analyzing these acceleration data. This paper describes resultant in-orbit deployment characteristics and latch-shock behavior of the two main reflectors and compares them with the results of ground testing, analysis, and verification. Data on latching status and thermal histories are also described. The accuracy and significance of ground validation methods are discussed.

Antenna Configuration and Deployment Mechanisms

Large Deployable Main Reflectors

Figure 1 shows the antenna configuration of ETS-VI. ETS-VI is a large-capacity multibeam CS using 13 beams in the 20–30-GHz frequency band and five beams in the 2.5–2.6-GHz frequency band. It has two large deployable main reflectors and two deployable subreflectors.[6] The largest reflector, which is 3.5 m in aperture, is divided into three portions. The small outer portions (called wing parts) are folded and fixed to the tower structure during launch. The other main reflector, which is 2.5 m in aperture, and the subreflectors are simply folded around hinge axes. They are fixed to the tower

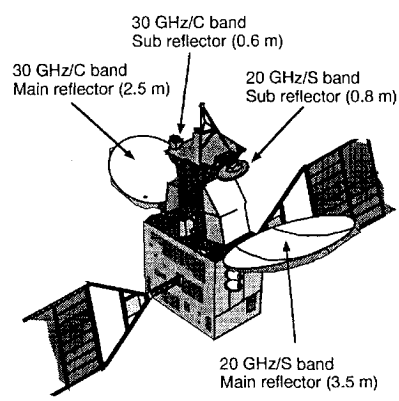

Fig. 1 Antenna configuration of ETS-VI.

Received April 30, 1995; revision received Oct. 10, 1995; accepted for publication Nov. 2, 1995.

*Senior Research Engineer, Satellite Communication Systems Laboratory, NTT Wireless Systems Laboratories, 1-2356 Take, Yokosuka-shi. Member AIAA.

Table 1 Allowable final deployment velocity[a]

Mechanism	Final velocity, rad/s	
	Allowable	Predicted
Wing part	1.76	1.10
3.5-m main refl.	0.20	0.11
2.5-m main refl.	1.00	0.30

[a]Failure mode: fracture of material in a truss member.

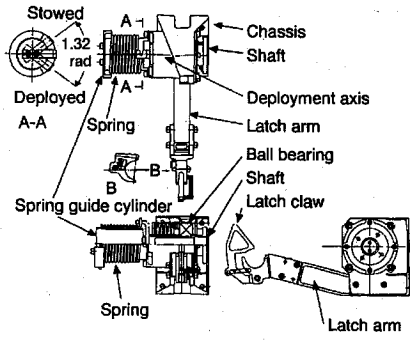

Fig. 2 Deployment mechanism for 3.5-m antenna.

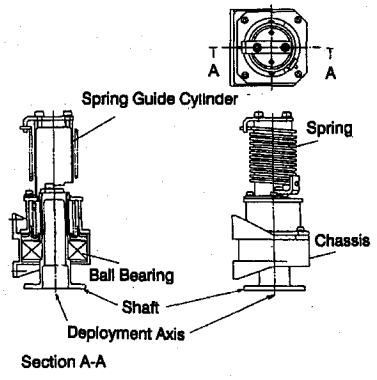

Fig. 3 Wing deployment mechanism for 3.5-m antenna.

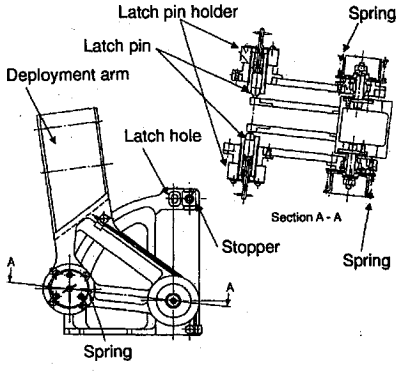

Fig. 4 Deployment mechanism for 2.5-m antenna.

structure by explosive bolts and nuts and released by deployment command.

Deployment Mechanisms

Figures 2 and 3 show the 3.5-m-antenna deployment mechanism and partial deployment (wing deployment) mechanism, respectively. These deployment mechanisms consist of ball bearings, a helical spring, a spring guide cylinder, a deployment axis, and a chassis. The wing deployment mechanism is installed in the upper and lower hinges between the wing parts and the central part. Figure 4 shows the 2.5-m-antenna deployment mechanism. Although there are some differences in detail between deployment mechanisms, such as the bearings and latch mechanisms, they share the same design concept. Each deployment mechanism is driven by a helical spring without any damping mechanism. Because of its simplicity, the driving mechanism has high deployment reliability. Large deployment torque produces high reliability. However, excessive torque causes structural destruction. Therefore, we must design the optimal deployment torque considering both structural strength and deployment reliability. For these antennas, the final deployment velocity is restricted by the truss members. Table 1 shows the allowable final deployment velocity for each deployment mechanism.

Ground Tests and Their Results

Figure 5 summarizes the ground test procedures in ETS-VI program. Ground testing was composed of several test programs. Each program was performed at four development levels: the mechanical parts level, mechanism assembly level, antenna component level, and system level. The final checkout work was performed at Tanegashima Space Center just before launch.

Mechanical Parts and Assembly

The most fundamental data are the characteristics of mechanical parts such as the spring torque, friction torque, cable bending moment, and resistant torque due to latch mechanisms. These data were measured in various test conditions assuming an in-orbit environment, and their characteristics were estimated statistically. Deployment reliability was estimated by using these characteristics.[7] In addition, the structural strength against latching shock was evaluated. At the mechanical assembly level, the variation of characteristics of mechanical parts against assembly process and test environment was measured. It was confirmed that the deployment characteristics of the mechanical assembly agreed with those predicted from the mechanical parts characteristics. Table 2 shows the torque budget of each deployment mechanism as obtained by mechanism assembly tests.

Antenna Component and System

At the antenna component and system levels, exact simulation of in-orbit motion was significantly inhibited by prominent gravitational and atmospheric effects. Ground deployment tests must be performed in limited configurations. Therefore, we developed gravity cancellation methods and equipment for each test configuration.[8,9] Air drag effects and gravity cancellation errors were quantitatively estimated. Furthermore, we estimated deployment characteristics by evaluating system parameters in a nonlinear equation for deployment motion using ground test results.[1] Deployment characteristics can be retrieved by using common deployment

Table 2 Driving torque characteristics

Mechanism	Driving torque, N m		Torque constant, N m/rad	
	Mean value	Standard deviation	Mean value	Standard deviation
$-Y$ wing part	2.605	0.121	−0.805	0.160
$+Y$ wing part	2.289	0.154	−0.773	0.189
3.5-m main refl.	1.274	0.200	−0.558	0.030
2.5-m main refl.	1.498	0.147	−0.292	0.147

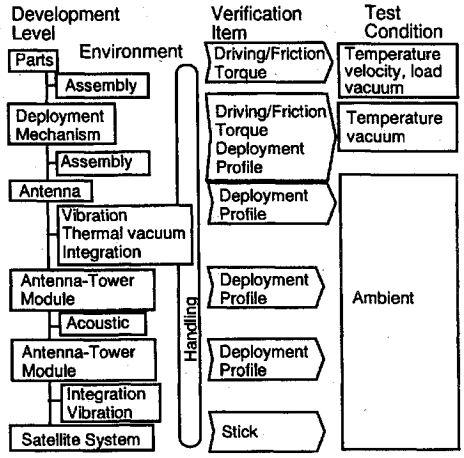

Fig. 5 Ground deployment test procedure in ETS-VI project.

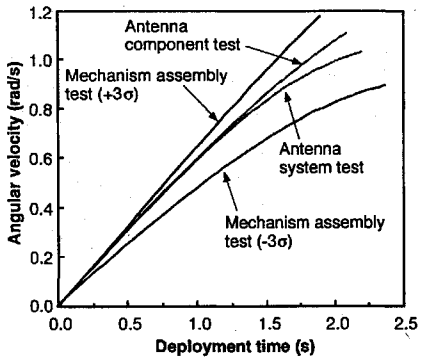

Fig. 6 Ground deployment test results.

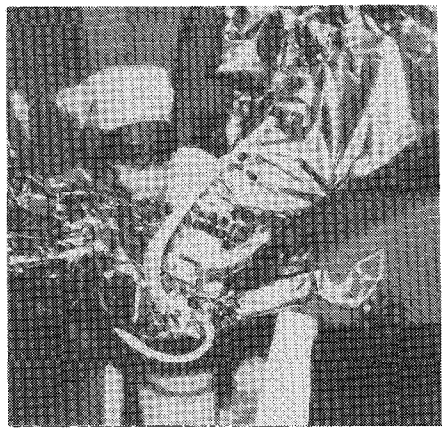

Fig. 7 Final setup configuration for 3.5-m-antenna deployment mechanism.

parameters such as the generalized driving torque, restricting torque, air damping coefficient, and so on.

The deployment parameters determined from ground testing on each development level can be used to show the variation of deployment characteristics through the assembly processes and test environments. Figure 6 shows the resultant angular velocity profile of wing deployment as compared with the mechanisms' assembly characteristics. It was confirmed that the wing deployment mechanisms maintained their design performance after testing and handling.

Not only did we consider the characteristics of deployment mechanisms, but we also inspected for interference between deployment mechanisms and other flight items installed near the mechanisms, such as wires and thermal blankets. Figure 7 shows a photograph of the final setup configuration around one of the 3.5-m antenna deployment mechanisms. Four months before launch, we performed final inspection at Tanegashima Space Center. At this time, we found some interference between thermal blankets and mechanisms. Such imprecision in structural design must be eliminated.

In-Orbit Deployment Sequence and Results

Thermal Environment

The most important observation items (telemetry items) in flight operations are the temperatures of deployment mechanisms, release mechanisms, and latch mechanisms. The critical temperature limits were calculated from thermal models. Allowable lower and upper temperature limits were determined by adding margins of analysis on the critical temperature limits. We must consider both the absolute temperature and the temperature difference between mechanical parts. Deployment mechanisms, release mechanisms, and latch mechanisms were tested within the critical absolute temperature range. The allowable temperature difference was determined by a gap between inner and outer bearing rings set in the deployment axis. Table 3 shows the critical absolute temperature and the temperature difference for each deployment mechanism. A larger temperature difference is allowed for the deployment mechanisms of the wing parts in the 3.5-m antenna, because the wing parts have a long hinge span, a short deployment arm, and many latch mechanisms. Figures 8 and 9 show the absolute temperature profile and

Table 3 Temperature requirements for antenna deployment mechanisms[a]

Mechanism	Temperature, °C Lower	Upper	Temp. diff., °C
$-Y$ wing	−90	100	60
$+Y$ wing	−90	100	60
3.5-m main refl.	−90	100	25
2.5-m main refl.	−90	100	25
3.5-m small refl.	−90	100	25
2.5-m small refl.	−90	100	25

[a]Release mechanisms: −40 to 70°C.

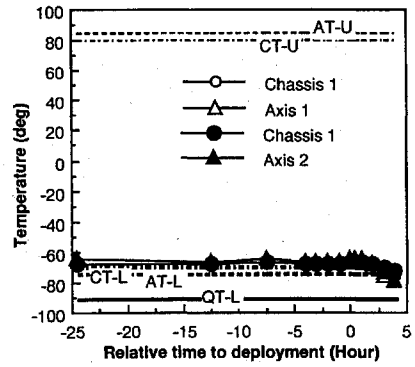

Fig. 8 Temperature profile of 3.5-m-antenna deployment mechanism.

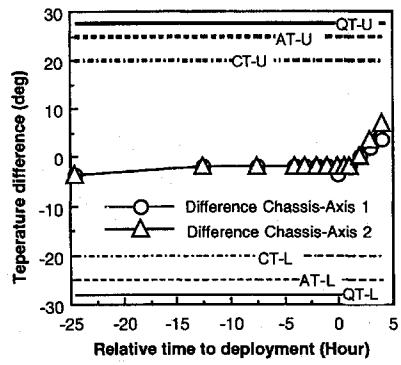

Fig. 9 Temperature difference profile of 3.5-m-antenna deployment mechanism.

the temperature difference profile of the deployment mechanisms for the 3.5-m antenna, respectively. The horizontal axis shows time relative to 3.5-m antenna deployment. The temperature limits are also shown as a caution level (CT-L), acceptance level (AT-L), and qualification level (QT-L). The 3.5-m antenna deployed in the lowest temperature condition.

Deployment Sequence and Results

Figure 10 shows the event sequence outline from liftoff to antenna deployment. ETS-VI was successfully launched on Aug. 28, 1994, from Tanegashima Space Center. After a few hours, temperature telemetry data were obtained and thermal control by using several film heaters began. ETS-VI was given the Japanese name Kiku-6 when the second stage of H2 rocket pushed out the satellite. Unfortunately, Kiku-6 could not be put into geostationary orbit because the liquid apogee propulsion subsystem failed. Thus Kiku-6 remained in an eccentric orbit, rotating around the sun-oriented axis, until all deployment appendages deployed to their predetermined positions. The deployment command for the wing parts of the 3.5-m antenna reflector was transmitted as the first event of antenna deployment. Surprisingly, the status of latch telemetry for the wing parts did not change from STOW to DEPLOY. The wing parts were expected to deploy in a few seconds; however, the status of telemetry was still STOW after a few minutes. The deployed status of the wing parts was, however, confirmed by the following circumstantial evidence: 1) the temperature of the wing part that would have been deployed toward the sun increased; 2) camera images of the wing part taken in the stowed configuration disappeared from

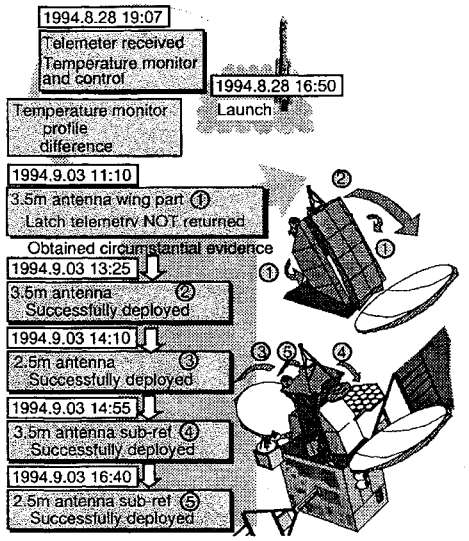

Fig. 10 Outline of event sequence.

the imaging data obtained by the onboard charge-coupled device camera; and 3) vibration caused by latching shock appeared in the dynamic response of the solar paddle, and the resulting measured deployment time of the wing part agreed with the predicted deployment time. Because of this evidence, we continued the deployment operations. Consequently, other deployments—2.5-m antenna and subreflectors—were successfully performed. Acceleration, temperature, and other flight data were also obtained by using some engineering sensors.

In-Orbit Deployment Performance

Deployment Analysis Model

For ground verification, a simple one-degree-of-freedom model was used to analyze deployment motion. This paper introduces a new deployment analysis model that considers the configuration of in-orbit acceleration measurement. Complicated multibody dynamics was dealt with by dynamic analysis and design system (DADS). Mass properties of the wing part of the 3.5-m antenna, the 3.5-m antenna itself, and 2.5-m antenna are shown in Table 4. As free-bending modes exist above 20 Hz, lower bending modes were determined by the elasticity of the deployment mechanisms. It was assumed that the elasticity of the 3.5-m antenna structure can be approximated as a revolutional spring in the following manner:

$$k_\theta = \frac{(2\pi f)^2}{I} \tag{1}$$

The wing parts of the 3.5-m antenna were treated as rigid bodies. Figure 11 shows an analysis model for antenna deployment created by DADS. Solar paddles and other appendages are not considered in this model. Latch mechanisms are considered as discontinuous constrained conditions.

Measurement System

The measurement system for the antenna reflectors consists of thermocouples, acceleration meters, and microswitches. Figure 12 shows the acceleration meter installed on the top of the antenna reflector structure. In contrast with the other telemeters, the acceleration data were accommodated in the launch environment measure. The resolution, range, and frequency response of the sensor are ± 10 mg, 200 μV dc ($1.0 \times 10^{-6} g$), and 30 Hz, respectively. The sampling time interval and accuracy of the obtained data were $\frac{1}{24}$ s and 8 bits, respectively. The microswitches indicate deployed status upon completion of latchup. They were installed in latch mechanisms as indicated in Fig. 2.

Resultant Deployment Performance

Obtained In-Orbit Data

Figure 13 shows the acceleration profile of the 3.5-m antenna during deployment and after latching up. The profile can be divided into two portions: free motion during deployment, and vibration excited by the latching shock. Three kinds of in-orbit characteristics can be retrieved from the acceleration profile. They are the characteristics of the deployment mechanisms, the influence of the elasticity of antenna structures on deployment motion, and the vibration characteristics of antenna structure in the deployed configuration.

Table 4 Mass properties

Mechanism	Mass, kg	Moment of inertia, kg m^2	Distance between hinge axis and c.g., m	Deployment angle, rad
$-Y$ wing part	8.90	2.30	0.503	1.280
$+Y$ wing part	8.90	2.30	0.503	1.227
3.5-m main refl.	39.80	273.4	2.21	1.274
2.5-m main refl.	19.55	49.95	1.25	1.344

Table 5 Predicted and measured deployment time

Event	Measured deployment time, s	Predicted deployment time, s				
		-2σ	-1σ	Mean	$+1\sigma$	$+2\sigma$
$-Y$ wing part	2.0[a]	2.1	2.0	1.9	1.9	1.8
$+Y$ wing part	2.0[a]	2.2	2.1	2.0	1.9	1.9
3.5-m main refl.	20.0	26.5	23.5	21.4	19.7	18.4
2.5-m main refl.	8.9	11.2	10.3	9.7	9.1	8.6

[a] $+Y$ and $-Y$ cannot be distinguished.

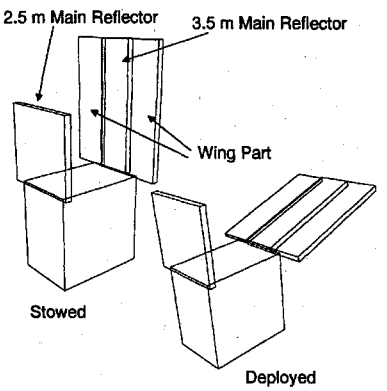

Fig. 11 Analytical model for antenna deployment created by DADS.

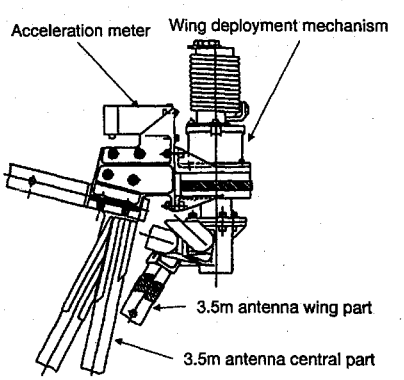

Fig. 12 Acceleration meter.

Measured and Predicted Deployment Time

Table 5 shows the measured deployment time in orbit compared with the predicted deployment time. The predicted deployment time was calculated by rigid multibody models using the mean values and standard deviations for the deployment mechanisms. As shown in the table, the measured deployment time agreed with the predicted deployment time within $\pm 1\sigma$ of mean values. Thus, it is seen that the characteristics of deployment mechanisms were verified properly by ground-deployment testing. The structural elasticity of this kind of antenna did not affect deployment time or final deployment velocity.

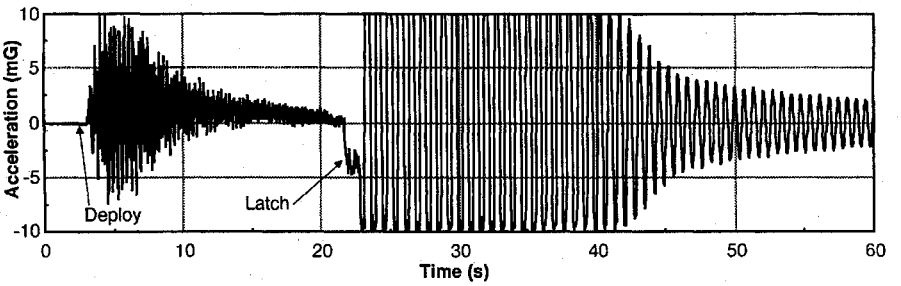

Fig. 13 Acceleration profile of 3.5-m antenna in orbit.

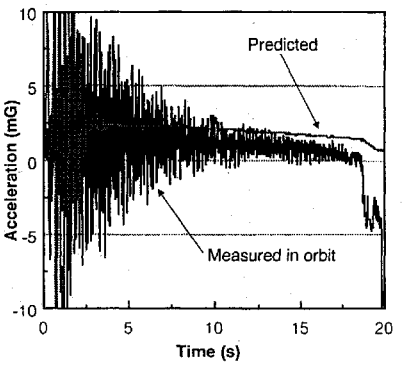

Fig. 14 Measured and predicted acceleration profile in orbit (3.5-m antenna).

Measured and Predicted Deployment Profile

Figure 14 shows the measured acceleration profile compared with the predicted profile calculated by the previously described analysis models. Because the predicted profile was calculated using mean values of the deployment torque, acceleration levels are slightly different from those in the measured profile.

Vibration Characteristics

Assuming that the dynamic response of the antenna reflectors after latchup can be modeled by a simple damped vibration, vibration characteristics of antenna structures can be estimated as follows.

The equation of damped oscillation for a single degree of freedom is

$$x = A\sin(\omega t + \phi)\, e^{-c\beta t} \tag{2}$$

$$\dot{x} = \omega A\cos(\omega t + \phi)\, e^{-c\beta t} + c\beta A\sin(\omega t + \phi)\, e^{-c\beta t}$$

$$= \beta\sqrt{1 - c^2}A\cos(\omega t + \phi)\, e^{-c\beta t} + c\beta A\sin(\omega t + \phi)\, e^{-c\beta t}$$

$$= A\beta e^{-c\beta t}\cos(\omega t + \phi + \psi) \tag{3}$$

$$\ddot{x} = -A\beta^2 e^{-c\beta t}\sin(\omega t + \phi + \psi + \varphi) \tag{4}$$

These vibration parameters can be estimated by fitting a calculated curve to the measured acceleration profile.

In-Orbit Vibration Characteristics

Figure 15 shows damped oscillation of the 3.5-m antenna in orbit as measured by the acceleration meter. Table 6 shows vibration parameters estimated by the best fitted curve plotted in Fig. 15. Using the previously described analytical model and a mean value of the driving torque, the final angular velocity of the 3.5-m antenna was calculated to be 0.11 rad/s. The tangential velocity at the top of the antenna is calculated as

$$L\dot{\theta} = 4.4\text{ m} \times 0.11\text{ rad/s} \approx 0.48\text{ m/s} \tag{5}$$

Thus the amplitude of vibration at the top of the antenna is calculated using vibration frequency $f = 1.4$ Hz as

$$A = \frac{L\dot{\theta}_{\max}}{2\pi f} = \frac{0.48\text{ m/s}}{2 \times 3.14 \times 1.4\text{ Hz}} = 0.055\text{ m} \tag{6}$$

Table 6 Estimated vibration parameters for 3.5-m antenna in orbit

A, m	β, rad/s	$\Phi + \phi + \psi$, rad	C	ω, rad/s	f, Hz
0.13	8.9	9.7	0.023	8.9	1.4

Table 7 Vibration parameters estimated during subreflector deployment

A, m	β, rad/s	$\Phi + \phi + \psi$, rad	C	ω, rad/s	f, Hz
0.0033	8.9	0.94	0.020	8.9	1.4

Table 8 Estimated vibration parameters assuming damping ratio

A, m	β, rad/s	$\Phi + \phi + \psi$, rad	C	ω, rad/s	f, Hz
0.073	8.9	9.7	0.020	8.9	1.4

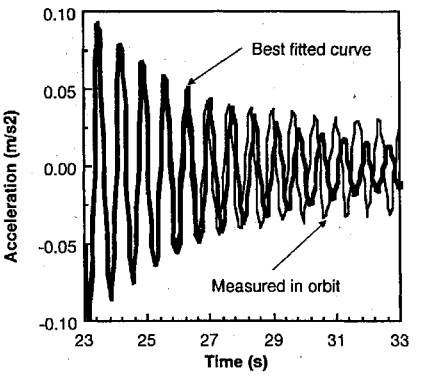

Fig. 15 Damped vibration in orbit (3.5-m antenna).

As shown in Table 6, the estimated vibration amplitude did not agree with the above simple calculation. The vibration profile may be affected by other appendages and the satellite attitude control system. The satellite attitude control system was planned to be suspended just before deployment and activated 30 s after the separation command. Considering that the deployment time duration is about 20 s and acceleration data were saturated for about 18 s, the resultant amplitude and damping ratios are not reliable. Table 7 shows vibration parameters estimated from acceleration data measured during deployment of the 20-GHz subreflector. These acceleration data were obtained within 15 s after the separation command. The damping ratio is slightly smaller than in Table 6. Using the damping ratio shown in Table 7, the vibration amplitude was reestimated as shown in Table 8.

Ground Latch Shock Testing

Ground latch shock testing was performed to verify the structural strength of the antenna against the latching shock of antenna deployment. An angular velocity sensor was installed in the deployment mechanism to measure the angular velocity profile. The angular velocity sensor can also show damped oscillation after latching up.

Table 9 Estimated vibration parameter for 3.5-m antenna on ground

A, m	β, rad/s	$\Phi+\phi+\psi$, rad	C	ω, rad/s	f, Hz
0.042	5.9	−0.23	0.10	5.9	0.94

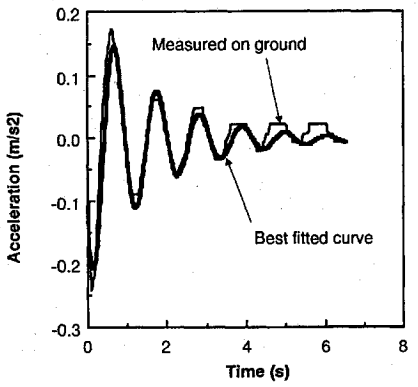

Fig. 16 Damped vibration on ground (3.5-m antenna).

To correct the final velocity for air drag, the antenna reflector was slightly accelerated by inclining the deployment axis. Figure 16 shows damped oscillation of the 3.5-m antenna on the ground, measured by the angular velocity sensor. The best fitted curve is also plotted. Table 9 shows estimated vibration parameters. The vibration frequency of 0.9 Hz agrees with the results of modal testing. The frequency reduction resulting from the air-mass effect on the first mode was estimated analytical to be 0.5 Hz (by NASTRAN). The obtained vibration frequency agrees with the in-orbit result. The final deployment angular velocity was measured to be 0.06 rad/s, and the vibration amplitude was calculated as

$$A = \frac{L\dot{\theta}}{\omega} = \frac{4.4 \times 0.06}{5.88} = 0.045 \text{ m} \tag{7}$$

Considering the air-mass effect, the vibration amplitude can be taken as

$$A = 0.042 \times \frac{0.11/0.06}{8.90/5.88} = 0.051 \text{ m} \tag{8}$$

This means that the dynamic response to the latching shock was slightly below that estimated. We must deal carefully with the damping ratio to verify the structural strength against latching shock. In this case, the structural strength of the 3.5-m antenna is sufficient. (The final angular velocity is 0.11 rad/s, as against an allowable maximum angular velocity of 0.2 rad/s.)

Feasibility and Reliability of Ground Validation Methods

Ground testing and verification were performed as follows: 1) acquisition of characteristics of mechanical parts and assemblies, 2) confirmation of deployment characteristics through the assembling and testing environments, 3) prediction of the in-orbit deployment performance by using characteristics of mechanical parts, and 4) evaluation of the structural strength of the antenna and dynamic loads at the interface to the satellite body by using deployment characteristics.

These testing and verification items were considered through the deployment analysis using rigid multibody dynamics and linear structural analysis. In addition, the gravity compensation system was found to offset the gravity force and torque within allowable cancellation errors, and these errors could be quantitatively estimated. Flight data obtained by in-orbit deployment measurements showed that these ground verification methods were feasible and reliable. The influence of elastic deformation on antenna deployment motion is negligibly small in the design of deployment mechanisms for this kind of solid antenna reflector. However, an anomaly was found in the microswitches for the deployment mechanisms. We assume that this was caused by local distortion due to some elastic deformation. For larger-scale antennas, we must consider nonlinear structural behavior and the dynamics of elastic structures.

Conclusion

In-orbit deployment characteristics were estimated by measuring the acceleration of the antenna reflector during and after deployment. By analyzing the obtained data and comparing them with the ground verification results, the following conclusions are drawn:

1) By ground-testing equipment using a suspension system and verification using system identification, one can precisely estimate in-orbit deployment characteristics.

2) Deployment reliability can be guaranteed by this ground verification method.

3) The dynamic response against latching shock was slightly under estimated by ground testing. Thus, we must deal carefully with the data obtained, considering the damping ratio used.

4) The structural elasticity of this kind of antenna does not affect deployment characteristics. However, we must be careful of local distortion.

Although ETS-VI could not perform the satellite communication experiments, its primary objectives such as antenna deployment and transponder performance were successfully confirmed. Thus, it was verified that our satellite communication technologies have reached the primary goal of the future advanced communication system. We have to make the best use of the lessons learned.

References

[1]Meguro, A., and Mitsugi, J., "Ground Verification of Deployment Dynamics of Large Space Structure Deployment," *Journal of Spacecraft and Rockets*, Vol. 29, No. 6, 1992, pp. 835–841.

[2]Stella, D., Morgant, F., and Nielsen, G., "Contraves Antenna Tip Hinge Mechanism for Selenia Spazio's 20/30 GHz Antenna," *Proceedings of the 2nd ESA Workshop on Mechanical Technology for Antennas*, European Space Agency, Paris, 1986, pp. 185–194.

[3]Martin, K., and De'Ath, D., "Evaluation from Hinge Actuator Mechanism to an Antenna Deployment Mechanism for Use on the European Large Communication Satellite (L-SAT/OLYMPUS)," *Proceedings of the 18th Aerospace Mechanism Symposium*, NASA-CP-2311, 1984, pp. 127–141.

[4]James, P. K., "Simulation of Deployment Dynamics for INTELSAT Transmit and Receive Boom/Antenna System," *COMSAT Technical Review*, Vol. 15, No. 1, 1985, pp. 127–141.

[5]Johnson, M. R., "The Galileo High Gain Antenna Deployment Anomaly," NASA-CP-3260, 1994, pp. 359–377.

[6]Minomo, M., and Yasaka, T., "Development of 30/20 GHz Satellite Antenna Structures," *Proceedings of ESA Workshop on Mechanical Technology for Antennas*, SP-261, European Space Agency, 1986, pp. 85–90.

[7]Misawa, M., Yasaka, T., and Shojiro, M., "Analytical and Experimental Investigation for Satellite Antenna Deployment Mechanism," *Journal of Spacecraft and Rockets*, Vol. 26, No. 3, 1989, pp. 181–187.

[8]Meguro, A., "Ground Testing Method for Large Deployable Antenna," *Proceedings of the 16th International Symposium on Space and Science*, AGNE Publishing, Tokyo, Japan, 1988, pp. 475–480.

[9]Meguro, A., "Considerations on Deployment Test Method for Large Satellite Antenna," *Proceedings of 1989 International Symposium on Antennas and Propagation*, Vol. 1, IEICE, Tokyo, Japan, 1989, pp. 85–88.

H. R. Anderson
Associate Editor